



Synthesis of nano hydroxyapatite from *Hypophthalmichthys molitrix* (silver carp) bone waste by two different methods: a comparative biophysical and in vitro evaluation on osteoblast MG63 cell lines

Prakruti Acharya · Manjushree Kupendra · Aneesa Fasim ·
K. S. Anantharaju · Nagaraju Kottam · V. Krishna Murthy ·
Sunil Shivajirao More 

Received: 25 April 2022 / Accepted: 9 August 2022 / Published online: 23 August 2022
© The Author(s), under exclusive licence to Springer Nature B.V. 2022

Abstract More than a thousand tonnes of fish bone wastes can be transformed into biomedical products annually. Alkaline hydrolysis and thermal calcification were used to create nanosized hydroxyapatite (HAp) crystals from Silver carp bone wastes. Biophysical tests were used to determine the nano size and chemical composition of synthesised hydroxyapatite. Alkaline hydrolysis hydroxyapatite (AH-HAp) was 58.3 nm, while Thermal calcination hydroxyapatite (TC-HAp) was 64.3 nm in size, confirmed by Atomic Force Microscopy. Energy Dispersive X-ray Analysis studies showed Ca/P (Calcium phosphate) ratio of AH-HAp to be 1.65, whereas TC-HAp as 1.45, confirming AH-HAp to be organically rich along with a similar Ca/P ratio as natural HAp. Fourier Transform Infrared Spectroscopy spectra indicated HAp formation from both procedures, however AH-HAp had superior crystallinity than TC-HAp confirmed from X-Ray Diffraction

spectra. MG63 osteoblast cell lines showed 91% cell viability in cytotoxicity studies and 70.1% proliferation efficiency in Alkaline Phosphatase assay, which was higher than TC-HAp. The present study shows that HAp produced via alkaline hydrolysis has better biocompatibility which enhances its applicability as a biomaterial, than HAp synthesized through thermal calcination, which tends to incinerate organic moieties.

Keywords Alkaline-hydrolysis · Biophysical-characterisation · *In vitro* osteoblast proliferation · Nano-hydroxyapatite · Thermal-calcination

Introduction

Hydroxyapatite ($\text{Ca}_{10}(\text{PO}_4)_6(\text{OH})_2$), a calcium phosphate ceramic is an integral part of bone and teeth in living beings is widely used as a biomaterial due to its non-toxic, non-inflammatory and nonimmunogenic behaviours (Barakat et al. 2009; Sossa et al. 2018). Individually porous and dense HAp with a stoichiometric molar ratio of Ca/P to be 1.67 have been dynamically studied and examined as implant materials for dental and orthopaedic purposes as they display significantly good osteoconductivity/inductivity (Boutinguiza et al. 2012). There is plenty of research ongoing currently regarding the production of proficient quality of HAp demonstrating substantial biocompatible properties along with an economical

P. Acharya · M. Kupendra · A. Fasim · V. K. Murthy ·
S. S. More (✉)
School of Basic and Applied Sciences, Dayananda Sagar
University Bangalore, Bangalore, Karnataka 560111, India
e-mail: sunilsmorey@gmail.com

K. S. Anantharaju
Department of Chemistry, Dayananda Sagar College
of Engineering, Bangalore, Karnataka 560111, India

N. Kottam
Department of Chemistry, M S Ramaiah Institute
of Technology, Bangalore, Karnataka 560054, India

and eco-friendly production methods. Nano scale hydroxyapatite can be manufactured from synthetic (chemical precipitation, hydrothermal, sol–gel methods) and natural sources (chicken, bovine and fish waste) (Sadat-Shojai et al. 2013). However, the lack of Fe^{2+} , Mg^{2+} , Si^{2+} , Na^+ , F^- ions, a distinguishing property of the osseous apatite, is a major drawback of HA produced via chemical synthesis along with the processes being complicated and also it removes the carbonate groups which negatively affects biological properties of HAp (Akindoyo et al. 2017; Sossa et al. 2018). HAp obtained from animal bones offers the benefit to conserve a handful properties of the precursor material like the intact structure and its chemical composition (Boutinguiza et al. 2012).

After understanding the HAp preparation from natural sources is advantageous, research on standardising the protocol in order to get maximum yield and retain the crystal properties is of dire need. Sintering the bone sources in dry or wet air from 800 to 1200 °C is currently followed as they retain the crystallinity and functional groups, but they do possess certain disadvantages as at extreme temperatures HAp loses its OH groups progressively and gets converted to oxyapatite rendering its loss of hydroxyapatite phase (Venkatesan et al. 2011). On the other hand, employing alkaline hydrolysis method to produce biologically compatible HAp from bone waste has drawn attention since it involves usage of less harmful chemicals and yet aids in greater yield with retainment of chemical structure. A comparative analysis between the two methods signifies the novelty of the work in understanding which process gives a better yield with properties to be retained.

An estimation of more than 91 million tons of fishes are trapped every year across the world and out of which only 50–60% of it is used for human consumption food due to its recommended nutritional values and easy accessibility, while rest is discarded as waste as per FAO reports (Boutinguiza et al. 2012; Salim). Hence, a generous amount of waste that includes scales, bones and skin are discarded which needs a suitable mode of processing that are major source for calcium and phosphate content from which hydroxyapatite can be derived (Deb et al. 2019). On the foundation of these study reports, in our current research, we have recognised the source of HAp to be from *Hypophthalmichthys molitrix* (Silver carp) fish bone waste. Abundant studies have been conducted to produce HAp from different

natural sources like cuttlefish (*Sepia officinalis*), sword fish (*Xiphias gladius*), Japanese sea bream, tuna (*Thunnus thynnus*) fish, *sardinia longiceps*, Salmon fishes (Venkatesan et al. 2015; Sunil and Jagannatham 2016; Surya et al. 2021). Silver carp fish is one of the major commercial fish species of India, especially along the Southern part of India and are extensively used as a food source. To the best of our knowledge, very less research on silver carp fish waste recycle has been conducted and also no specific reports on synthesis of HAp from it has been achieved yet, however different methodologies have been used to extract only calcium components from the same source (Yin et al. 2017). Therefore, the principal purpose of our study was to synthesize nano-range HAp from Silver carp bone waste and contribute in neutralizing the caused pollution. Consequently, this waste can be used as raw materials in biomedical and regenerative medicines as an alternative to synthetically produced HAp. Two different approaches to isolate nano hydroxyapatite from silver carp bones were followed, the alkaline hydrolysis method: a new technique to isolate HAp and thermal calcination method: traditional way of isolation of hydroxyapatite. The extracted and synthesised nano HAp have been characterised and compared through biophysical spectral studies, and also examined for its biocompatibilities in utilisation of the biomaterial in various biomedical engineering fields.

Materials and methods

Sample collection

The disposed silver carp fish waste was collected and bought in an ice box from a nearby market area from Bangalore city, Karnataka, India and refrigerated at $-20\text{ }^\circ\text{C}$ until the next step of experimental design. Further these bones were separated from the collected silver carp flesh adhered around using cutter, scels and cleansed.

Preparation of n-hydroxyapatite

Alkaline hydrolysis method

Surya et al., (2021) and (Venkatesan et al. 2015) protocol was followed in the extraction of hydroxyapatite from bones via Alkaline hydrolysis method with slight modifications. The separated and cleansed bones were

dried and boiled for 1 h with 2L of distilled water to remove the remaining adhered skin and flesh. These bones were then transferred into 250 ml of 2% NaOH and 10 ml of acetone mixed solution and boiled for 1 h for the removal of additional lipids and proteins along with other organic impurities. The washed bones were placed in sterile hot air oven at 80 °C for 2 h for complete evaporation of moisture. The dried bones were cooled and later crushed by means of a mortar and pestle.

The pre-treated crushed bone powders were further again treated with 5% NaOH solution and boiled at 70 °C with continuous stirring at 400 rpm for 3 h. Later, the obtained powder was filtered and the precipitate was rinsed with double distilled water several times till a clear white precipitate was obtained, the pH of the solution was set to 7 with 0.1 M H₃PO₄. The washed precipitate was desiccated at 80 °C in a sterile hot air oven for 1 h to obtain dry hydroxyapatite (HAp) powder.

Calcination method

For the calcination process, the bone samples were cleaned and desiccated in a sterile hot air oven at 80 °C for 1 h to wash away the moisture content. After the drying process, these bones were slightly crushed and placed in a ceramic crucible that was subsequently heated in a muffle furnace at 900 °C for 3 h with controlled heating system maintained at 10 °C/min to obtain hydroxyapatite crystals. Further the powder was cooled slowly to room temperature (Abifarin et al. 2019).

Percent yield

The percent yield of isolated HAp from both the methods were calculated to determine and deduce an optimum method. It was calculated based on the formula (Hasan et al. 2020),

$$\text{Yield \%} = \frac{\text{Weight of HAp in gms}}{\text{Weight of Bones in gms}} \times 100$$

Biophysical characterisations of AH-HAp and TC-HAp samples

FTIR spectrum analysis

Fourier transformed infrared spectroscopy (Thermo Fischer Scientific) was performed for both the samples in the range of 400–4000 cm⁻¹. Background scan and sample scan were consecutively measured at a resolution of 4 cm⁻¹ and 2.8 mm/sec mirror speed for a total of ten scans. The synthesised samples were placed on the diamond crystal and clamped using pressure gauges. Prior to background data collection, the spectral data of test samples were recorded and the functional groups present were identified and analysed (Esmaeilkhanian et al. 2019).

XRD analysis

The phase and crystallinity of both the synthesised HAp powders were evaluated using an X-ray diffractometer with a 2θ range of 5°–70° using a Rigaku D/Max X-ray diffractometer with Cu Kα radiation source with a wavelength of 1.54 Å and scanning rate maintained at 10° min⁻¹. The current and voltage was set to 120 mA and 40 kV respectively (Mir et al. 2012).

Atomic force microscopy

The surface roughness, morphology, and crystals size estimation were observed using atomic force microscopy A-100 AFM (APE Research, Italy) for HAp samples operating in contact mode. The cantilevers have a spring constant k=0.03 Nm⁻¹ and tip curvature radius R=235 nm. For a stronger and better understanding of the particles 2D and 3D pictures of the samples were also collected accordingly (Jaber et al. 2018).

EDX analysis

To account the chemical composition of AH-HAp and TC-HAp, Energy dispersive X-ray spectroscopy (EDX) technique (8100-Shimadzu) was employed

and the Calcium/Phosphate ratio (Ca/P) was calculated accordingly (Granito et al. 2018).

SEM analysis

Surface morphological studies of AH-HAp and TC-HAp was carried out using scanning electron microscope (SEM). HAp crystals were layered with gold and was studied with magnification of 1000X and 3000X (S-4700, Hitachi Ltd., Tokyo, Japan). The interfaces were surveyed in secondary electron mode at 1 keV accelerating voltage and 10 mA emission current.

In vitro studies

Haemolytic assay

Haemolytic testing of synthesised HAp powders was performed according to ISO 10993–4 protocol. 5 ml of human blood was collected from a volunteer with consent from institution's ethical committee and diluted 40 folds with saline water. Different concentrations of test samples (AH-HAp and TC-HAp) were incubated with 1 ml of prepared diluted blood at 37 °C for 60 min. Triton100X with PBS and PBS alone were taken as positive and negative control respectively. Post incubation period, centrifugation was carried out at 280×g for 10 min and absorbance was noted at 540 nm using UV/Visible spectrophotometer. The percentage of haemolysis was calculated using below mentioned formula:

$$\text{Hemolysis}\% = \left(\frac{O.D_{\text{sample}}}{O.D_{\text{blank}}} \right) \times 100$$

MTT assay

Cytotoxicity and viability of MG63 osteoblast cell lines were determined using the 3-(4, 5-dimethylthiazol-2-yl)-2, 5-diphenyl tetrazolium bromide MTT assay. MG63 osteoblast cells (1×10^5 cell/ml) were seeded on 96 well plates containing DMEM (Dulbecco's Modified Eagle Medium) media with 10% Foetal bovine serum and incubated at 37 °C for 24 h. The different concentration of AH-HAp and TC-HAp (62.5–500 µg/ml) was added to the wells containing cells and followed by an additional 24 h

of incubation. After the incubation period, the culture media was decanted and fresh media comprising MTT reagent (0.5 mg/ml) was added followed by incubation of the plate for 5 h prior addition of 100 µl of DMSO (Dimethylsulfoxide). The absorbance at 570 nm was measured using a Biorad microplate reader (Aramwit et al. 2010).

Alkaline phosphatase (ALP) activity

100 µl of the diluted cell suspension (50,000 cells/well) was added to 96 well plates and incubated for 24 h under standard conditions. After the formation of monolayer, the media was decanted and further rinsed with fresh media. To this 100 µl of various concentration of AH-HAp and TC-HAp were added. The culture plates were further incubated for 24 h at 37 °C in 5% CO₂ atmosphere. Post incubation, 50 µl working reagent containing 0.32 mmol/L of 2- Amino 2-Methyl-Propanol, 1 mmol/L of Zn SO₄, 4 mmol/L of Magnesium Acetate along with 10 mmol/ of PNPP (p-nitrophenyl phosphate) was added to 50 µl of test solutions. Absorbance was noted at 405 nm every 1 min. ALP activity was determined using below mentioned formula,

$$\text{ALP activity} = \Delta \text{Absorbance}^{-1} \text{ min} \times 2720$$

$$\Delta \text{Absorbance}^{-1} \text{ min} = \text{Mean absorbance change per min.}$$

Alamar blue assay

MG63 osteoblast cell lines (5×10^5 cells/ml) were added to 96 well plate and allowed to form a monolayer at 37 °C for 24 h with 5% CO₂ supplied constantly. Once the monolayer was formed, media was decanted and fresh media containing different test concentrations was incubated following by addition of 20 µl of Alamar blue reagent. The plates were incubated at 37 °C in 5% CO₂ incubator for 4 h. Fluorescence was measured at excitation wavelength of 560 nm and an emission wavelength of 590 nm. The proliferation was represented as percentage and was calculated based on the RFU values obtained.

Statistical analysis

All experimental trials were conducted in triplicates. The graphs are represented as \pm mean standard errors bar with respective subsets. To ascertain the significance level ($p < 0.05$) of obtained results one way ANOVA and post hoc Tukey's test was conducted using SPSS software version 28.0.

Results and discussion

Percentage yield

Percentage yield of HAp from both the methods were calculated to determine the weight of extracted test samples irrespective of the methods. Dry weights of bones were noted prior the treatments and the weight of the obtained powder were noted as well. 69.9% of HAp was obtained from Alkaline hydrolysis, while a comparatively lower percent of 50.1% of HAp was obtained from the thermal calcination method. However, the obtained percent yield of HAp powders from thermal calcination and alkaline hydrolysis methods were in close accordance with (Barakat et al. 2009; Afridah et al. 2021) reports confirming the extraction efficiency. Nevertheless, the yield obtained from alkaline hydrolysis method was higher than the yield from thermal calcination signifying its efficiency in methodology. The possible explanation for higher yield could be due to retained organic moieties in this method when compared to that of calcination techniques (Venkatesan et al. 2011).

Biophysical characterisation of hydroxyapatite (HAp) – AH-HAp and TC-HAp

FTIR spectral analysis of AH-HAp and TC-HAp

Structural investigations of specific functional groups were identified using FTIR absorbance profile. Figure 1 represent the normal transmittance-FTIR spectra of HAp from both proposed methods. Distinguishing bands corresponding to carbonate groups (CaCO_3), a major component of hydroxyapatite is located at 1408 cm^{-1} for both the powders because of the aromatics C–C and N–O stretching (Surya et al. 2021) which additionally confirms the synthesis of hydroxyapatite. These bands are also indicative of

formation of B-Type apatite by replacement of phosphate ions with carbonate ions (Abifarin et al. 2019). They also specify that the CO_3^{2-} groups are free from organic matter, thus authenticating the elimination of organic part and the presence of carbonated HAp crystals (Venkatesan et al. 2011). Another, determinative pointer of HAp was in the form of a pronounced sharp band at 1012 cm^{-1} and at 1020 cm^{-1} for AH-HAp and TC-HAp respectively describing the asymmetric stretching mode of vibration of PO_4 group. As well, the bands between 560 and 600 cm^{-1} match to symmetric P–O stretching vibration of PO_4 group that was very much evident in both the synthesised powders. Additionally, as an added confirmation no traces for acid phosphate (HPO_4^{2-}) was observed as there were no visible peaks around 540 – 530 cm^{-1} that are considered to be characteristic peaks for undeveloped bone mineral or incomplete apatite phase (Farmer 1974). These obtained bands were compared and found to be similar with the HAp spectrum in different studies (Gergely et al. 2010; Abifarin et al. 2019). The study revealed the isolation of carbonated hydroxyapatite and also the similarities of FTIR spectral data from both methods. These synthesised carbonated HAp from our study display possible beneficial applications in tissue engineering with good biocompatibility, osteointegration, high osteoconductivity as the mineral phase of bone is majorly composed of carbonated HAp (Venkatesan et al. 2011).

XRD spectral analysis of AH-HAp and TC-HAp

XRD is an effective qualitative and quantitative technique used to analyse the crystalline phases in materials. The XRD pattern obtained from AH-HAp and TC-HAp are displayed in Fig. 2. It has been reported that the biological response of HAp depends on its physicochemical properties, including crystal size and composition. Acceptance rate in tissue engineering will be higher if the synthesised HAp exhibits similarity in size and crystal dimensions to that of human bone tissue. The XRD pattern of the AH-HAp exhibited the characteristic planes of hydroxyapatite including a high intensity peak at 31.9° corresponding to 211 plane along with 002, 102, 210, 211, 112, 300, 202, 301, 212, 203, 222, 312, 213, 321 planes while TC-HAp also displayed high intensity peak at 31.9° and all other similar peaks as of AH-HAp. The spectral pattern

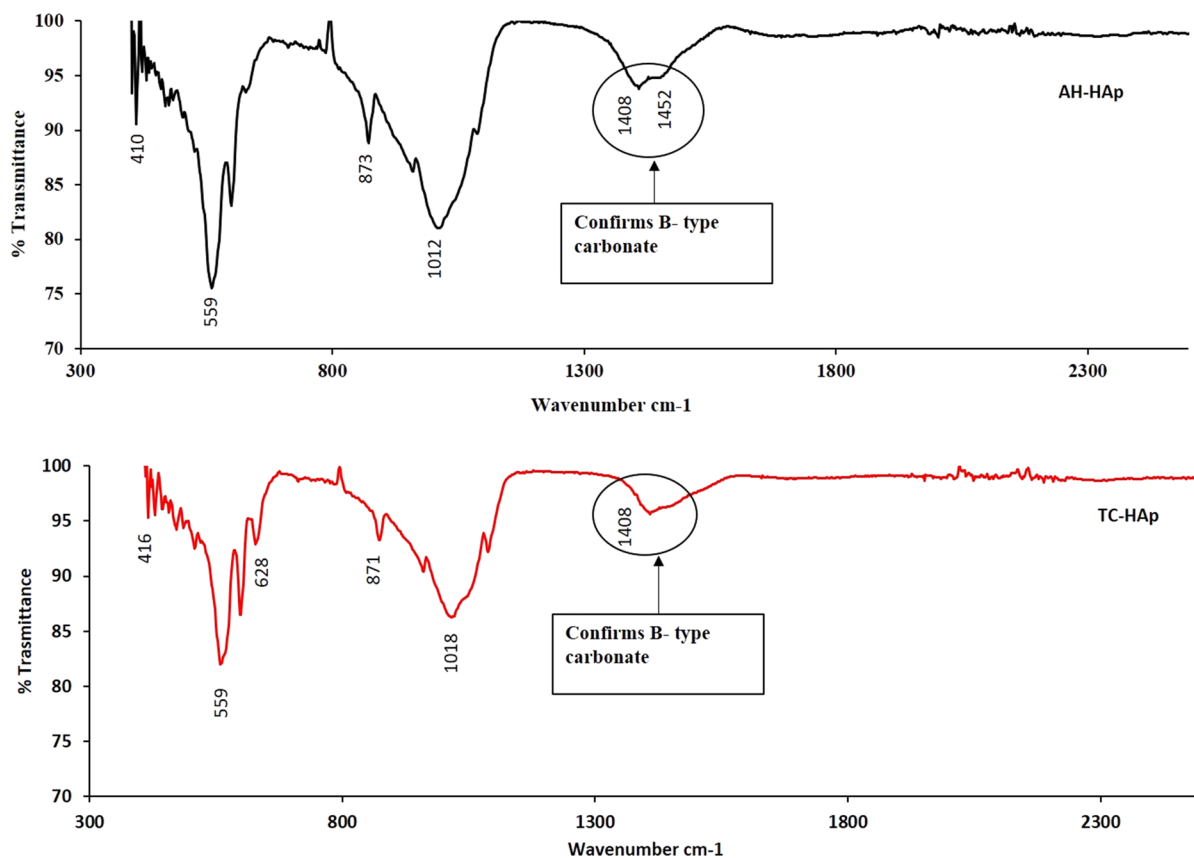


Fig. 1 FTIR Spectral graphs of AH-HAp and TC-HAp: characteristic HAp peaks with a carbonate peak at 1408 cm^{-1} confirms the formation of B-type apatite

from both the methods were matched with JCPDS 9–0432 file corresponding to Hydroxyapatite which confirmed that the crystals of HAp had no impurities and was purely hydroxyapatite. However, a noticeable pattern in XRD spectra is the sharpness of the obtained peaks in TC-HAp which is related to the removal of organic moieties due to increased temperature treatment. The spectral pattern of AH-HAp has lesser sharper peaks comparatively confirming the retainment of the organic content. Also, the increased peak width of AH-HAp and the decreased peak width of TC-HAp indicates that size of crystals acquired from alkaline hydrolysis technique is likely smaller in comparison with thermal calcination technique (Venkatesan et al. 2011; Mustafa et al. 2015). Hence it can be inferred that Alkaline hydrolysis treatment is comparatively a better procedure as it has not influenced the chemical structure of hydroxyapatite and also has retained

its organic moieties which will assist in providing better osseointegration when used as a raw material in the biomedical industry.

Atomic force microscopy studies of AH-HAp and TC-HAp

The crystal size of AH-HAp and TC-HAp was tested to confirm the nanophase structure and is shown in Fig. 3. As per the results of atomic force microscopy, the average size of crystals of AH-HAp was found to be 58.3 nm (Max size: 196.6 nm) while TC-HAp crystals had an average size of 64.3 nm (Max size: 256.5 nm). Size determination is an important criterion in understanding its utilisation as a raw material in the bone tissue engineering field. From the AFM studies, it clearly justifies that HAp synthesised from the alkaline hydrolysis method with a lower crystal size displays greater applicability in the biomedical field as

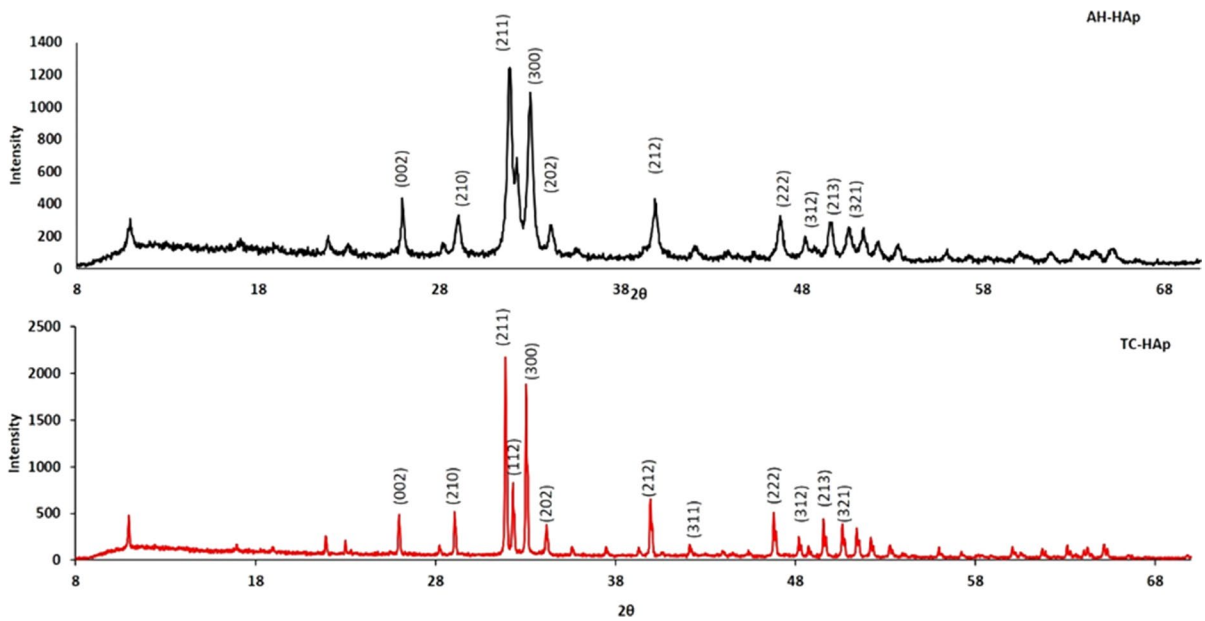


Fig. 2 XRD spectral graphs of AH-HAp and TC-HAp: Characteristic HAp planes matching with JCPDS 9–0432 file, along with a high intensity peak at 32° (211)

it can facilitate greater cell to surface interaction and act as a better osteoconductive agent (Rios-Pimentel et al. 2019). In thermal calcination technique, due to high temperatures the crystal agglomeration takes place leading to increased size, while this is avoided in alkaline hydrolysis method that possibly helped in retaining the crystal size in a lower nano range (Venkatesan et al. 2011).

EDX analysis of AH-HAp and TC-HAp

In order to establish the synthesis of hydroxyapatite from the proposed methods, electron diffraction X-ray analysis was performed (Fig. 4). The Ca/P ratio is nearly 1.67, which defines the chemical formula of the standard hydroxyapatite (Barakat et al. 2009). The Ca/P ratio of AH-HAp and TC-HAp was determined to be 1.65 and 1.45 respectively from EDX reports. The different states of apatite stages present in HAp include calcium phosphates such as amorphous calcium phosphates, brushite ($\text{CaHPO}_4 \cdot 2\text{H}_2\text{O}$), monetite (CaHPO_4), tricalcium phosphate [$\text{Ca}_3(\text{PO}_4)_2$] (TCP), α -TCP and β -TCP, and hydroxyapatite. The Ca/P ratio of these are 0.5, 1.0, 1.3, 1.5 and 1.67 respectively (Fiume et al. 2021). Ca/P ratio of AH-HAp is matching to the 1.67 value for its pure hydroxyapatite state

than TC-HAp which still is in an intermediate step towards the formation of HAp. However, observation of small amount of Na and Mg ions in EDX results of HAp is in accordance with the published studies. Also, occurrence of Mg is beneficial as these Mg ions is one of the essential micronutrient that is necessary for tissue metabolic events (Sunil and Jagannatham 2016). The results illustrate that the synthesised HAp from silver carp fish waste by following alkaline hydrolysis method is in its pure form with stoichiometric Ca/P ratio that can be used as a capable bio ceramic material in the medical engineering fields.

SEM analysis of AH-HAp and TC-HAp

The SEM micrographs of TC-HAp and AH-HAp at 1000 \times and 3000 \times magnification are illustrated in Fig. 5. Crystals of AH-HAp displayed a conserved rod like and flaky structures due to the possible occurrence of collagen type 1, an organic material which could have retained in alkaline hydrolysis method that is visible in SEM results. The crystals of TC-HAp displayed a powdery image that explains the agglomeration due to its formation at higher temperatures. From this investigation, we can conclude that AH-HAp in its nano range with its organic constituents

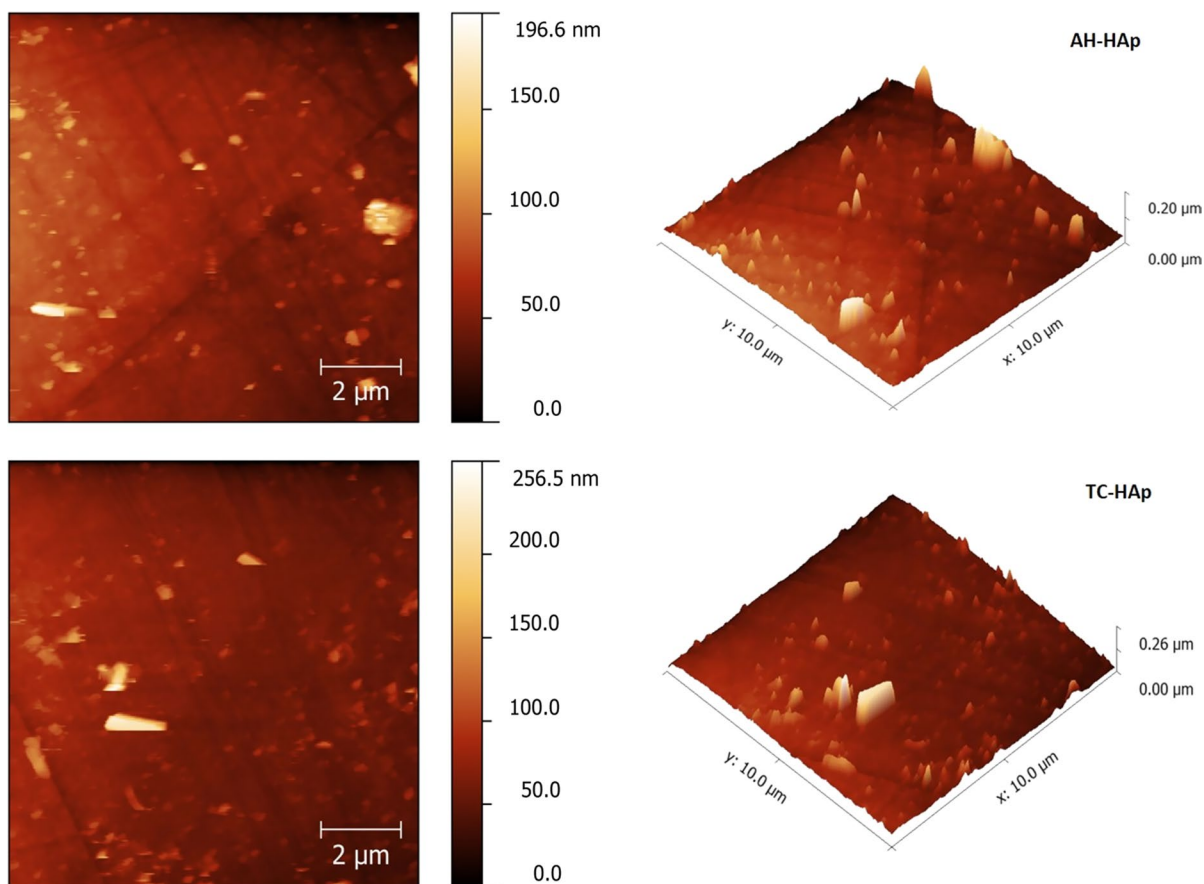


Fig. 3 AFM profile of AH-HAp and TC-HAp: Nano crystals of AH-HAp are in the range of 50–196 nm, while TC-HAp ranged from 60 to 256.5 nm

facilitates better properties as a bioactive component in bone scaffolds as regenerative medicines in its native form.

Invitro studies of AH-HAp and TC-HAp

Haemolytic activity of AH-HAp and TC-HAp

The invitro blood compatibility of AH-HAp and TC-HAp at different concentrations was done according to ASTM F756-00 that classifies, test components displaying haemolytic activity below 5% as non-haemolytic (non-toxic) and anything higher than 5% to be haemolytic (toxic). It is significant to determine the haemolytic potency of any component, particularly a nanoparticle that has to be administered in the human body. Table 1 shows that AH-HAp displayed 2.24, 2.30, 3.19, 3.23, 3.35% of haemolysis while

TC-HAp displayed 3.94, 4.78, 5.12, 7.76, 9.22% of haemolysis at increasing concentrations. TC-HAp has showed more haemolytic (toxic) activity than AH-HAp. Reports have suggested that synthetic HAp and TC-HAp display toxicity (Jadalannagari et al. 2014; Palanivelu and Ruban Kumar 2014) compared to AH-HAp which is coinciding with our data. The good hemocompatibility nature of AH-HAp confirms us that it is nontoxic and can be used as drug system for a human body.

MTT assay

To evaluate the cell viability and proliferation of AH-HAp and TC-HAp, the MTT assay on MG63 cells were carried out and images have been displayed at all concentrations describing the growth pattern (Fig. 6 and 7). It is observed that AH-HAp from

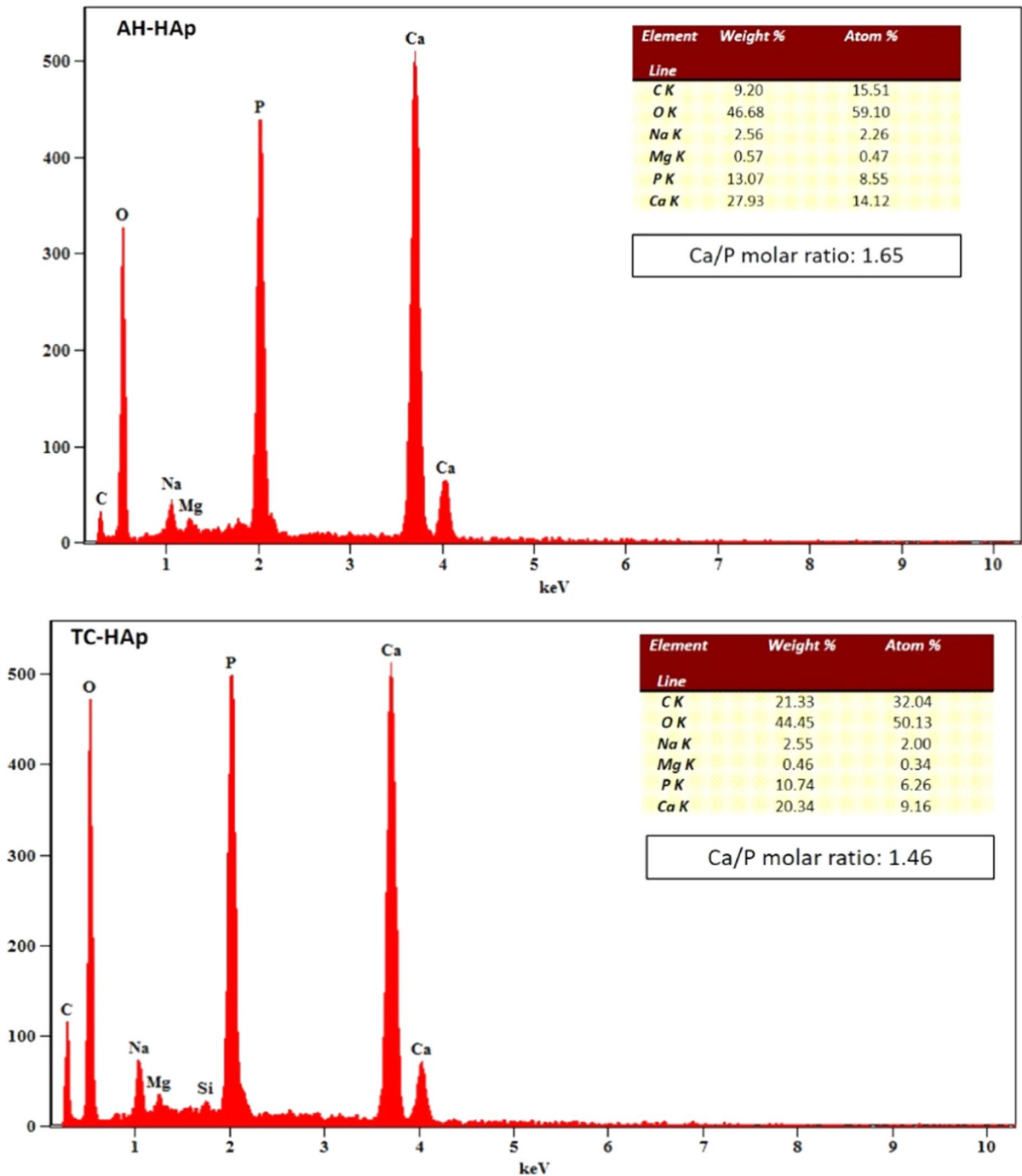


Fig. 4 EDX spectral graphs of AH-HAp and TC-HAp: Ca/P ratio of AH-HAp and TC-HAp was determined to be 1.65 and 1.45 respectively

fish bone significantly promoted 91% of cell viability at a concentration of 500 µg/ml, while TC-HAp displayed 86% of viability at same concentration.

Previously, (Sathiskumar et al. 2019) has reported synthesis of nano hydroxyapatite from *Cirrhinus mrigala* fish waste and its viability was checked at lower

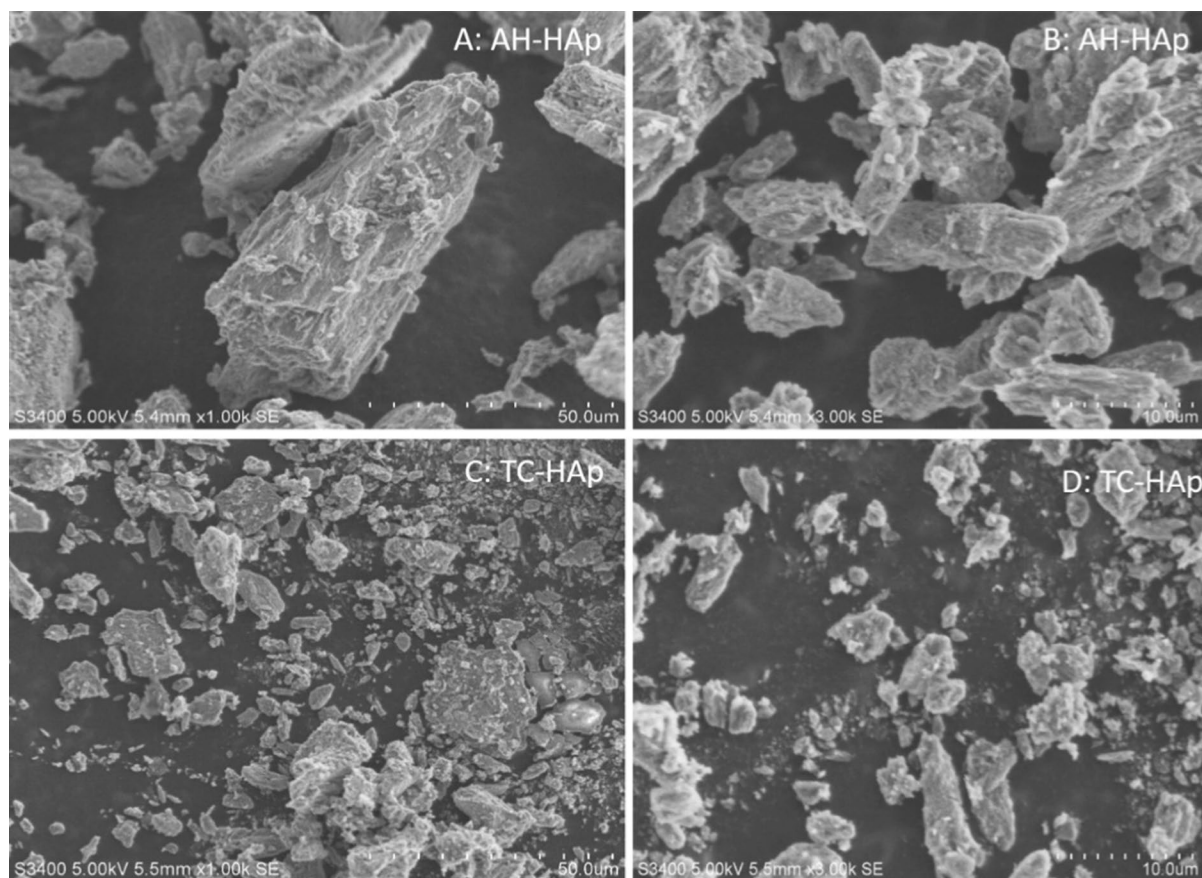


Fig. 5 SEM micrographs of AH-HAP and TC-HAP: A and B – micrographs of AH-HAP at 1000X and 3000X; C and C- micrographs of TC-HAP at 1000X and 3000X

concentration (5–100 $\mu\text{g/ml}$), however our reports suggest higher percent of viability at higher concentration confirming the efficiency of the synthesised products. The chief influencing factor in cell viability of MG 63 cells are source of bone extracted, its

Table 1 Percent Haemolysis of AH-HAP and TC-HAP: 3.35% of haemolysis was observed from AH-HAP while, 9.22% from TC-HAP made its lightly toxic in comparison with AH-HAP

HAp Conc. (mg/ml)	AH-HAP % haemolysis	TC-HAP % haemolysis
1	2.24 ± 0.016	3.94 ± 0.003
2	2.30 ± 0.026	4.78 ± 0.007
3	3.19 ± 0.021	5.12 ± 0.010
4	3.23 ± 0.021	7.76 ± 0.009
5	3.35 ± 0.003	9.22 ± 0.0076

density, flexibility, crystallization, porosity with element composition (Li et al. 2012). It is also reported that the presence of CO_3^{2-} , Mg^{2+} group and crystalline structure of HAp influences the cell adhesion and promotion of cells under in vitro conditions (Shi et al. 2018). These results indicated that AH-HAP have positive affect on differentiation of osteoblast making it a novel component in bone regeneration.

Alamar blue assay

Metabolic activity of AH-HAP and TC-HAP on MG63 cell lines are displayed in Fig. 8. with different concentrations. AH-HAP treated cells showed a significant cell proliferation of 20% ($p < 0.001$) compared to TC-HAP treated cells showing 15% ($p < 0.001$) at final concentration (250 mg/ml). Our reports are in accordance with (Shor et al. 2007; Yu

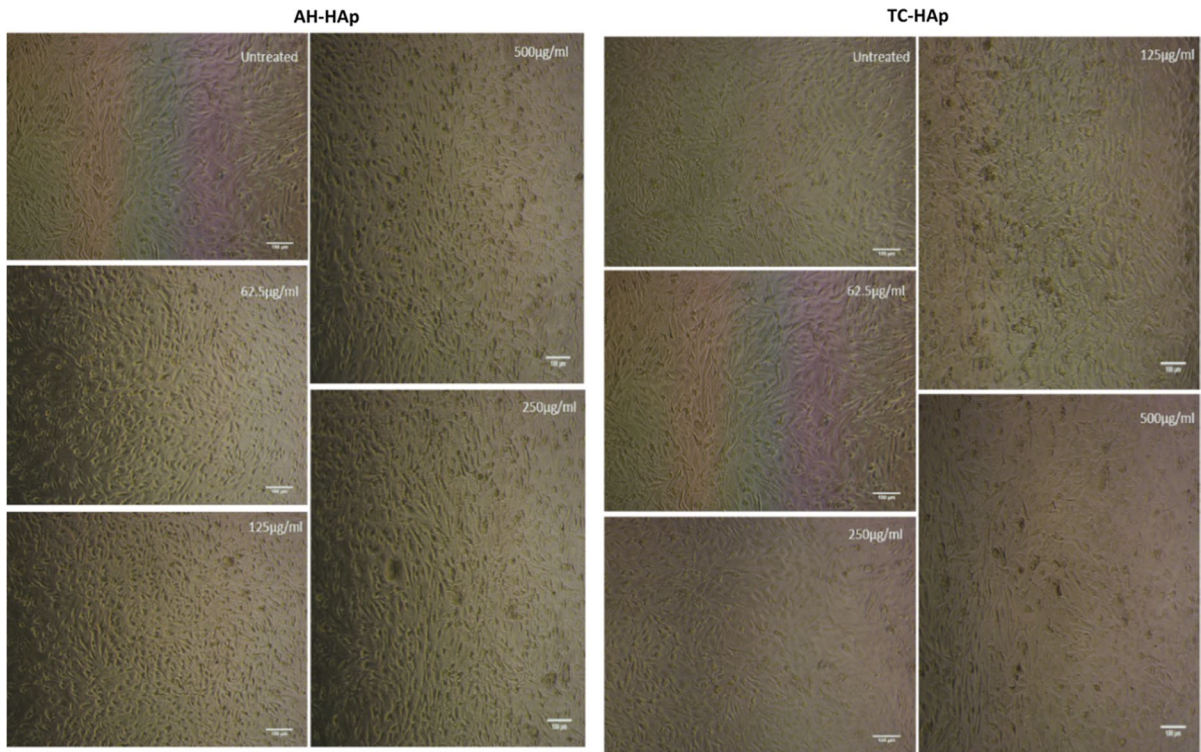


Fig. 6 Adhesion pattern of MG63 osteoblast cell lines on AH-Hap and TC-Hap: cell lines on AH-Hap coated dishes at different concentrations showed better adhesion than TC-Hap determining the comparatively higher toxicity levels of TC-Hap

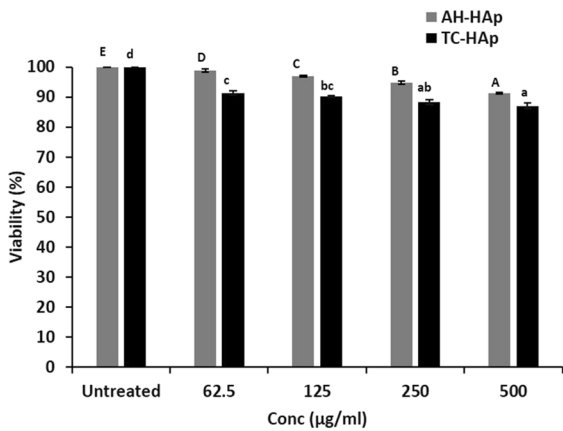


Fig. 7 Cell viability (%) of AH-Hap and TC-Hap: Cytotoxicity of AH-Hap and TC-Hap was evaluated using MG63 cell lines. Cells without samples are denoted as untreated, test samples as AH-Hap and TC-Hap displayed 91% and 86% viability at highest concentration of 500 µg/ml. The obtained results ($n=3$)±SD were found to be statistically significant ($p<0.001$)

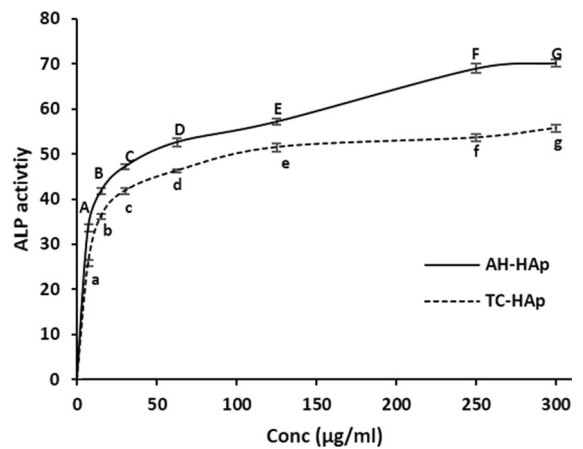


Fig. 8 ALP activity of AH-Hap and TC-Hap: Percentage proliferation of AH-Hap and TC-Hap was determined on MG63 cell lines with varying concentration. AH-Hap showed greater ALP activity (70.1%) compared to TC-Hap (56.8%) at final concentration of 300 µg/ml. The obtained results ($n=3$)±SD were found to be statistically significant ($p<0.001$)

et al. 2009; Cozza et al. 2018) having similar cell proliferation activity from PCL/hydroxyapatite and natural hydroxyapatite from cuttlefish bone respectively confirming the biocompatibility of the synthesised material. HAp composition containing calcium, sodium and phosphate play chief role in bone formation and bone resorption (Ducheyne and Qiu 1999). During bone remodulation, activation of the intracellular mechanism, metabolic processes in bone formation and calcification is involved by the presence of calcium and silicone molecules (Hoppe et al. 2011). Thus, HAp from natural bone source with retainment of its native properties is proven to have the ability to proliferate cells that leads in new bone formation and resorption.

Alkaline phosphatase activity

MG63 cell line culture is used to check the activity of ALP to evaluate the ability of bone cells to differentiate and proliferate in presence of AH-HAp and TC-HAp. Figure 9 display the ALP activity of MG63 cultured on AH-HAp and TC-HAp as substrate. From the obtained results we could observe that ALP activity on AH-HAp was much higher (70.1%) than that of TC-HAp (56.8%) activity during the incubation period. This can be attributed to the stronger interaction between AH-HAp and osteoblast cells in comparison with TC-HAp ($p < 0.005$). Our reports show significantly higher ALP activity compared to other

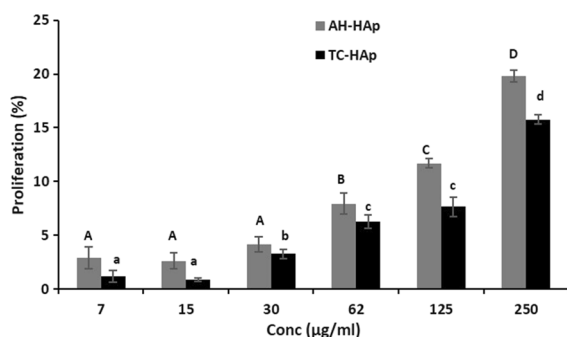


Fig. 9 Percentage proliferation of AH-HAp and TC-HAp: Alamar blue assay was conducted to determine the % proliferation of AH-HAp and TC-HAp at different concentrations. 20% proliferation was displayed by AH-HAp and TC-HAp showed 15% at a highest concentration of 250 µg/ml. The obtained results ($n=3$) \pm SD were found to be statistically significant ($p < 0.001$)

reports (Ramires et al. 2001; Ressler et al. 2018). It is reported that skeletal bone development requires the right amount of osteoblast proliferation and differentiation that modulates various signalling pathways. From our result outcome, it is understood that AH-HAp has facilitated increased proliferation indicating increased ALP activity as Alkaline phosphate is a pointer of the osteoblastic phenotype and is expressed only when differentiation of osteoblasts occur from progenitor cells (Huang et al. 2011). Therefore, T-HAp is an ideal material that can be used in bone repair and hence can be used in fabrication of scaffold for bone regeneration and development.

Conclusion

Powders of AH-HAp and TC-HAp were synthesized using thermal calcination and alkaline hydrolysis methods. Our findings suggested that AH-HAp revealed better structural properties and was well within the nano scale limit in comparison with TC-HAp as per the AFM studies. On the other hand, XRD analysis helped us to notice that both HAp crystals displayed single phase and FTIR results showed typical functional group peaks confirming the extraction efficiency of both the proposed methods. Nevertheless, AH-HAp offered better crystallinity suitable for biological applications than the TC-HAp. Ca/P ratio of 1.67 was observed in AH-HAp, while TC-HAp displayed lesser Ca/P ratio. The biocompatibility tests including MTT, ALP and Alamar blue assays of AH-HAp compared with TC-HAp have shown higher cell viability and biocompatibility confirming the effectiveness of the alkaline hydrolysis synthesis method. In a nutshell, it can be established that alkaline hydrolysis is the best suitable methodology for synthesis of HAp in nano scale than the thermal calcination technique. The proposed hydrolysis technique in the study has a benefit in synthesising hydroxyapatite with essential physio-chemical and bioactive characteristics like size, morphology, functional groups and viability suitable for bone regeneration applications. Additionally, due to its superior osteoconductive capability, synthesised HAp can be greatly favoured in Bone Tissue engineering applications, where it is presently the most prevalent commercial product utilised in clinical research.

Future prospects

In the field of regenerative medicine, the HAp is becoming increasingly important as a potential alternative for autograft due to its unique properties. The synthesised hydroxyapatite has characteristics that can be efficiently utilised in bone tissue engineering as a biocompatible material in various treatments of ortho and dental applications. The way HAp works with tissues is important. It is vital to recognize how the host reacts to HAp. In general, the way a biomaterial works is by being biocompatible, biotolerant, bioinert, bioactive. Hence, *in vivo* studies of the samples will strengthen the study and our findings to substantiate its utilisation in preparations of scaffolds which will again require investigation of surface morphology, pore architecture and mechanical properties to justify its cytotoxicity and its applications in various other biotechnological fields.

Acknowledgements The authors would like to thank Dayananda Sagar University and M S Ramaiah Institute for providing lab facilities. The authors report no funding for this manuscript.

Funding The authors have not disclosed any funding.

Declarations

Conflict of interest The authors have not disclosed any competing interests.

References

- Abifarín JK, Obada DO, Dauda ET, Doodoo-Arhin D (2019) Experimental data on the characterization of hydroxyapatite synthesized from biowastes. *Data Brief* 26:104485. <https://doi.org/10.1016/j.dib.2019.104485>
- Afridah W, Wikurendra EA, Amalia R, Syafiuddin A (2021) Synthesis and Characterization of Hydroxyapatite Derived from Milkfish Bone by Simple Heat Treatments. *J Mater Sci Eng* 203:012003. <https://doi.org/10.1088/1757-899X/203/1/012003>
- Aramwit P, Kanokpanont S, Nakpheng T, Srichana T (2010) The effect of sericin from various extraction methods on cell viability and collagen production. *Int J Mol Sci* 11:2200–2211. <https://doi.org/10.3390/ijms11052200>
- Barakat NAM, Khil MS, Omran AM et al (2009) Extraction of pure natural hydroxyapatite from the bovine bones bio waste by three different methods. *J Mater Process Technol* 209:3408–3415. <https://doi.org/10.1016/j.jmatprotec.2008.07.040>
- Boutinguiza M, Pou J, Comesaña R et al (2012) Biological hydroxyapatite obtained from fish bones. *Mater Sci Eng, C* 32:478–486. <https://doi.org/10.1016/j.msec.2011.11.021>
- Cozza N, Monte F, Bonani W et al (2018) Bioactivity and mineralization of natural hydroxyapatite from cuttlefish bone and Bioglass® co-sintered bioceramics. *J Tissue Eng Regen Med*. <https://doi.org/10.1002/term.2448>
- Deb P, Barua E, Das Lala S, Deoghare AB (2019) Synthesis of hydroxyapatite from Labeo rohita fish scale for biomedical application. *Mater Today Proc* 15:277–283. <https://doi.org/10.1016/j.matpr.2019.05.006>
- Ducheyne P, Qiu Q (1999) Bioactive ceramics: the effect of surface reactivity on bone formation and bone cell function. *Biomaterials* 20:2287–2303. [https://doi.org/10.1016/s0142-9612\(99\)00181-7](https://doi.org/10.1016/s0142-9612(99)00181-7)
- Esmailkhanian A, Sharifianjazi F, Abouchenari A et al (2019) Synthesis and characterization of natural nano-hydroxyapatite derived from turkey femur-bone waste. *Appl Biochem Biotechnol* 189:919–932. <https://doi.org/10.1007/s12010-019-03046-6>
- Farmer VC (1974) The infrared spectra of minerals. Mineralogical Society of Great Britain and Ireland, London
- Fiume E, Magnaterra G, Rahdar A et al (2021) Hydroxyapatite for biomedical applications: a short overview. *Ceramics* 4:542–563
- Gergely G, Wéber F, Lukács I et al (2010) Preparation and characterization of hydroxyapatite from eggshell. *Ceram Int* 36:803–806. <https://doi.org/10.1016/j.ceramint.2009.09.020>
- Granito RN, Renno ACM, Yamamura H et al (2018) Hydroxyapatite from fish for bone tissue engineering: a promising approach. *Int J Mol Cell Med* 7(2):80. <https://doi.org/10.2208/IJMCM.BUMS.7.2.80>
- Hasan MR, Yasin NSM, Mohd MS (2020) proximate and morphological characteristics of nano hydroxyapatite (nano hap) extracted from fish bone. *J Sustain Sci Manag* 15:9–21. <https://doi.org/10.4675/jssm.2020.12.002>
- Hoppe A, Güldal NS, Boccaccini AR (2011) A review of the biological response to ionic dissolution products from bioactive glasses and glass-ceramics. *Biomaterials* 32:2757–2774. <https://doi.org/10.1016/j.biomaterials.2011.01.004>
- Huang Y-C, Hsiao P-C, Chai H-J (2011) Hydroxyapatite extracted from fish scale: effects on MG63 osteoblast-like cells. *Ceram Int* 37:1825–1831. <https://doi.org/10.1016/j.ceramint.2011.01.018>
- Jaber HL, Hammood AS, Parvin N (2018) Synthesis and characterization of hydroxyapatite powder from natural Camelus bone. *J Aust Ceram Soc* 54:1–10. <https://doi.org/10.1007/s41779-017-0120-0>
- Jadalannagari S, Deshmukh K, Ramanan SR, Kowshik M (2014) Antimicrobial activity of hemocompatible silver doped hydroxyapatite nanoparticles synthesized by modified sol–gel technique. *Appl Nanosci* 4:133–141
- Li Q, Li M, Zhu P, Wei S (2012) In vitro synthesis of bioactive hydroxyapatite using sodium hyaluronate as a template. *J Mater Chem*. <https://doi.org/10.1039/C2JM33624C>

- Mir M, Leite FL, Herrmann Junior PSDP, Pissetti FL, Rossi AM, Moreira EL, Mascarenhas YP (2012) XRD, AFM, IR and TGA study of nanostructured hydroxyapatite. *Mat Res* 15:622–627. <https://doi.org/10.1590/S1516-14392012005000069>
- Mustafa N, Ibrahim MHI, Asmawi R, Amin AM (2015) Hydroxyapatite extracted from waste fish bones and scales via calcination method. *AMM* 773–774:287–290. <https://doi.org/10.4028/www.scientific.net/AMM.773-774.287>
- Palanivelu R, Ruban Kumar A (2014) Synthesis, characterization, in vitro anti-proliferative and hemolytic activity of hydroxyapatite. *Spectrochim Acta Part A Mol Biomol Spectrosc* 127:434–438. <https://doi.org/10.1016/j.saa.2014.02.106>
- Ramires PA, Romito A, Cosentino F, Milella E (2001) The influence of titania/hydroxyapatite composite coatings on in vitro osteoblasts behaviour. *Biomaterials* 22:1467–1474. [https://doi.org/10.1016/S0142-9612\(00\)00269-6](https://doi.org/10.1016/S0142-9612(00)00269-6)
- Ressler A, Ródenas-Rochina J, Ivanković M et al (2018) Injectable chitosan-hydroxyapatite hydrogels promote the osteogenic differentiation of mesenchymal stem cells. *Carbohydr Polym* 197:469–477. <https://doi.org/10.1016/j.carbpol.2018.06.029>
- Rios-Pimentel FF, Chang R, Webster TJ et al (2019) Greater osteoblast densities due to the addition of amphiphilic peptide nanoparticles to nano hydroxyapatite coatings. *IJN* 14:3265–3272. <https://doi.org/10.2147/IJN.S189323>
- Sadat-Shojai M, Khorasani M-T, Dinpanah-Khoshdargi E, Jamshidi A (2013) Synthesis methods for nanosized hydroxyapatite with diverse structures. *Acta Biomater* 9:7591–7621. <https://doi.org/10.1016/j.actbio.2013.04.012>
- Salim SS Fish consumption pattern in India, exports - Overview. 4
- Sathiskumar S, Vanaraj S, Sabarinathan D et al (2019) Green synthesis of biocompatible nanostructured hydroxyapatite from *Cirrhinus mrigala* fish scale – a biowaste to biomaterial. *Ceram Int* 45:7804–7810. <https://doi.org/10.1016/j.ceramint.2019.01.086>
- Shi P, Liu M, Fan F et al (2018) Characterization of natural hydroxyapatite originated from fish bone and its biocompatibility with osteoblasts. *Mater Sci Eng, C* 90:706–712. <https://doi.org/10.1016/j.msec.2018.04.026>
- Shor L, Güçeri S, Wen X et al (2007) Fabrication of three-dimensional polycaprolactone/hydroxyapatite tissue scaffolds and osteoblast-scaffold interactions in vitro. *Biomaterials* 28:5291–5297. <https://doi.org/10.1016/j.biomaterials.2007.08.018>
- Sossa PAF, Giraldo BS, Garcia BCG et al (2018) Comparative study between natural and synthetic Hydroxyapatite: structural, morphological and bioactivity properties. *Matéria (rio j)*. <https://doi.org/10.1590/s1517-707620180004.0551>
- Sunil BR, Jagannatham M (2016) Producing hydroxyapatite from fish bones by heat treatment. *Mater Lett* 185:411–414. <https://doi.org/10.1016/j.matlet.2016.09.039>
- Surya P, Nithin A, Sundaramanickam A, Sathish M (2021) Synthesis and characterization of nano-hydroxyapatite from *Sardinella longiceps* fish bone and its effects on human osteoblast bone cells. *J Mech Behav Biomed Mater* 119:104501. <https://doi.org/10.1016/j.jmbbm.2021.104501>
- Venkatesan J, Qian ZJ, Ryu B et al (2011) A comparative study of thermal calcination and an alkaline hydrolysis method in the isolation of hydroxyapatite from *Thunnus obesus* bone. *Biomed Mater* 6:035003. <https://doi.org/10.1088/1748-6041/6/3/035003>
- Venkatesan J, Lowe B, Manivasagan P et al (2015) Isolation and characterization of nano-hydroxyapatite from salmon fish bone. *Materials* 8:5426–5439. <https://doi.org/10.3390/ma8085253>
- Yin T, Park JW, Xiong S (2017) Effects of micron fish bone with different particle size on the properties of silver carp (*hypophthalmichthys molitrix*) surimi gels. *J Food Qual* 2017:e8078062. <https://doi.org/10.1155/2017/8078062>
- Yu H, Wooley PH, Yang S-Y (2009) Biocompatibility of Poly-ε-caprolactone-hydroxyapatite composite on mouse bone marrow-derived osteoblasts and endothelial cells. *J Orthop Surg Res* 4:5. <https://doi.org/10.1186/1749-799X-4-5>

Publisher's Note Springer Nature remains neutral with regard to jurisdictional claims in published maps and institutional affiliations.

Springer Nature or its licensor holds exclusive rights to this article under a publishing agreement with the author(s) or other rightsholder(s); author self-archiving of the accepted manuscript version of this article is solely governed by the terms of such publishing agreement and applicable law.